Stoichiometry of Recombinant N-Methyl-D-Aspartate Receptor Channels Inferred from Single-channel Current Patterns

Louis S. Premkumar and Anthony Auerbach

From the Department of Biophysical Sciences, State University of New York, Buffalo, New York 14214

ABSTRACT Single-channel currents were recorded from mouse NR1-NR2B (ζ-ϵ_2) receptors containing mixtures of wild-type and mutant subunits expressed in *Xenopus* oocytes. Mutant subunits had an asparagine-to-glutamine (N-to-Q) mutation at the N_0 site of the M2 segment (NR1:598, NR2B:589). Receptors with pure N or Q NR1 and NR2 subunits generated single-channel currents with distinctive current patterns. Based on main and sublevel amplitudes, occupancy probabilities, and lifetimes, four patterns of current were identified, corresponding to receptors with the following subunit compositions (NR1/NR2): N/N, N/Q, Q/N, and Q/Q. Only one current pattern was apparent for each composition. When a mixture of N and Q NR2 subunits was coexpressed with pure mutant NR1 subunits, three single-channel current patterns were apparent. One pattern was the same as Q/Q receptors and another was the same as Q/N receptors. The third, novel pattern presumably arose from hybrid receptors having both N and Q NR2 subunits. When a mixture of N and Q NR1 subunits was coexpressed with pure mutant NR2 subunits, six single-channel current patterns were apparent. One pattern was the same as Q/Q receptors and another was the same as N/Q receptors. The four novel patterns presumably arose from hybrid receptors having both N and Q NR1 subunits. The relative frequency of NR1 hybrid receptor current patterns depended on the relative amounts of Q and N subunits that were injected into the oocytes. The number of hybrid receptor patterns suggests that there are two NR2 subunits per receptor and is consistent with either three or five NR1 subunits per receptor, depending on whether or not the order of mutant and wild-type subunits influences the current pattern. When considered in relation to other studies, the most straightforward interpretation of the results is that *N*-methyl-D-aspartate receptors are pentamers composed of three NR1 and two NR2 subunits.

KEY WORDS: ion channel • subunits • subconductance • glutamate

INTRODUCTION

N-methyl-D-aspartate (NMDA)[1] receptors participate in excitatory synaptic transmission in the central nervous system and play an important role in the modulation of synaptic function (Hollmann and Heinemann, 1993; Bliss and Collingridge, 1993; McBain and Mayer, 1994). Two classes of NMDA receptor subunit have been cloned, called ζ and ϵ in the mouse, or NR1 and NR2 in the rat (Moriyoshi et al., 1991, Meguro et al., 1992; Monyer et al., 1992). Several lines of evidence indicate that native NMDA receptors are heteromultimers of both subunit classes. The coexpression of NR1 and NR2 subunits in *Xenopus* oocytes results in much larger currents compared with the expression of homomeric NR1 receptors (Nakanishi, 1992; Seeburg, 1993). In human embryonic kidney cells, NR1 subunits alone do not form functional channels (Grimwood et al., 1995). Further evidence suggesting that receptors are com-

prised of both subunit types is that NR1 and NR2 subunit-specific antibodies co-immunoprecipitate their antigens in the rat cortex (Sheng et al., 1994) and in transfected HEK cells (Chazot et al., 1994). With regard to receptor function, recombinant NR1/NR2B receptors exhibit a pattern of conductances (Stern et al., 1992), and have an equilibrium dissociation constant for MK801 (Chazot et al., 1994), similar to native receptors, suggesting that these two subunits coassemble.

The number of copies of the NR1 and NR2 subunit per receptor has not been clearly established. Kinetic and dose–response studies indicate that the activation of native NMDA receptors usually requires at least two molecules each of glycine and glutamate (Patneau and Mayer, 1990; Benvineste and Mayer, 1991; Clements and Westbrook, 1991). Glutamate binding appears to be associated with the NR2 subunit (Laube et al., 1997), and glycine binding with the NR1 subunit (Kuryatov et al.,1994; Hirai et al., 1996); thus, these studies suggest that NMDA receptors are at least tetramers comprised of two or more each of the NR1 and NR2 subunits. From analyses of single-channel current patterns of hybrid NR1-NR2A receptors, Behe et al. (1996) concluded that there are probably two copies of the NR1 subunit per receptor.

Address correspondence to Dr. Anthony Auerbach, Department of Biophysical Sciences, State University of New York, Buffalo, NY 14214. Fax: 716-829-2415; E-mail: auerbach@xenopus.med.buffalo.edu

[1]*Abbreviations used in this paper:* LL, log likelihood; N, asparagine; NMDA, *N*-methyl-D-aspartate; Q, glutamine.

Other non-NMDA glutamate receptors (GluR) appear to have five subunits. The apparent molecular weights of purified homomeric GluR receptor complexes are approximately five times that of a single subunit (Blackstone et al., 1992; Wenthold et al., 1992). In addition, an analysis of GluR1 receptors composed of subunits with mixed sensitivities to channel blockers suggests a pentameric stoichiometry (Ferrier-Montiel and Montal, 1996).

An asparagine-to-glutamine (N-to-Q) mutation at the N_0 position of the M2 segment (also called the QRN site) of NR1 and NR2B subunits (Burnashev et al., 1992; Kuner et al., 1996) generates receptors that have a prominent subconductance level (Ruppersberg et al., 1993; Premkumar and Auerbach, 1996a; Schneggenberger and Ascher, 1997). Here, we record single-channel currents from receptors comprised of mixtures of wild-type and N_0 mutant subunits. When the NR1 subunit is mixed and the NR2 subunit is purely mutant, six distinct current patterns are apparent. When the NR2 subunit is mixed and the NR1 subunit is purely mutant, only three current patterns are apparent. We conclude that recombinant NMDA receptors are probably pentamers composed of three NR1 and two NR2B subunits. Some results have been presented previously in abstract form (Premkumar and Auerbach, 1996b).

MATERIALS AND METHODS

Expression, Solutions, and Recording

The mouse subunit cDNAs were a generous gift from Prof. Masayoshi Mishina (Tokyo University, Tokyo, Japan). The injection and electrophysiology protocols are described in detail elsewhere (Methfessel et al., 1986; Premkumar and Auerbach, 1996a). Oocytes were taken from *Xenopus* anaesthetized by an intramuscular injection of 0.1 cc 2% MS-222. Although we studied receptors assembled from mouse subunits, we will refer to the subunits using the NR1/NR2B naming convention.

Briefly, oocytes were injected with 50 nl of RNA (1 μg/ml) for NR1 and NR2B. For each subunit class, either mutant (NR1:N598Q or NR2B:N589Q) or a mixture of mutant plus wild-type cRNAs were injected. Unless stated otherwise, the injection ratio for the mixtures was 1:1. Between 4 and 15 d after injection, oocytes were exposed to hypertonic solution to remove the vitelline layer. Single channel currents were recorded from excised outside-out patches (Hamill et al., 1981). Currents were activated by rapid (<2-ms exchange time) superfusion of 2–20 μM NMDA plus 10 μM glycine. Pipettes were filled with (mM): 90 Na-gluconate, 10 NaCl, 10 BAPTA, 10 HEPES, 2 K_2ATP, 0.25 GTP, pH 7.3. The extracellular solution contained (mM): 100 NaCl, 2.5 KCl, 5 HEPES, 1.5 or 5 EGTA, pH 7.3. Ultra-pure salts were obtained from Johnson Matthey (Ward Hill, MA). All experiments were performed at 22–25°C. Unless noted otherwise, the membrane potential was −80 mV.

Currents were recorded using an EPC-7 patch clamp amplifier (List Electronic, Darmstadt, Germany). Patches were superfused with the agonist solution for several minutes before recording in order to establish a steady state level of activity. The currents were digitized at 94 kHz and stored in video format (VR-10B; Instrutech Corp., Great Neck, NY). For analysis, the currents were filtered at 2 kHz (−3 db frequency with an 8-pole low pass Bessel filter; Frequency Devices, Haverhill, MA) and continuous current records (1–10 min in duration) were digitized at 5 kHz. All-point amplitude histograms were made for each of these continuous segments (see Fig. 1).

Defining Patterns and Clusters

Receptors with at least one mutant subunit had multiple open channel current levels. In most cases, the single-channel currents appeared to have one main (the largest amplitude) and one sublevel, although for some receptor assemblies two sublevels were apparent. For each assembly, a pattern of sub- and main level currents was defined by the amplitudes, standard deviations, lifetimes, and occupancy probabilities of the different current levels.

In experiments where both mutant and wild-type cDNAs were expressed for either the NR1 or NR2 subunit, multiple current patterns were often observed in a single patch. One goal of the analysis was to separate and quantify the distinct receptor assemblies according to their current patterns. An automated procedure was used to define, select, classify, and count the different current patterns.

The first step of this procedure was to break the continuous record into segments. All intervals between 2 and 12 pA were detected (program IPROC; Sachs, 1983). Next, clusters were defined as groups of openings separated by closed intervals less than some critical value, τ_{crit} (program LPROC; Neil et al., 1991). Ideally, the values of τ_{crit} should be determined from the distribution of closed intervals so that some shut components are completely included and others are completely excluded from the clusters. However, the closed interval distributions of NMDA receptors are complex, especially when several different receptor subtypes are present in the same patch, and no such clear separation could be accomplished. Kinetic analyses of patches apparently containing a single current pattern indicate that for each receptor subtype there is a closed interval component in the range ~6 ms (Premkumar et al., 1997). τ_{crit} was therefore set to 10 ms. Note that the subsequent classification of clusters is not sensitive to the precise value of τ_{crit} because the likelihood computed by the Viterbi algorithm is only weakly influenced by the closed-interval durations. However, the number of detected clusters of each pattern is sensitive to the value of τ_{crit}. If, for example, an occupied receptor can enter a closed state(s) for a period >10 ms, then activity before and after such a closure would be counted as two clusters even though it arose from a single activation. It is possible that different receptor compositions might enter such long-lived closed states with different probabilities. Therefore, we emphasize that the number of clusters of each current pattern does not necessarily reflect the number of receptors of that composition.

Next, a subset of detected clusters was selected for further analysis. To reject overlapping currents from multiple channels, only clusters having a mean amplitude (i.e., the average of all nonclosed levels) between −2 and −9 pA were accepted. Considering the pattern with the lowest average amplitude (N/Q; see Table III), the lower limit allowed the inclusion of a sublevel sojourn (−2.4 pA), and the upper limit led to rejection of two overlapping main level sojourns (−9.2 pA). To include enough main-subconductance transitions to allow pattern classification, only clusters having durations >10 (or in some cases 20) ms were selected for further analysis.
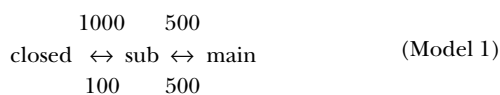
Classification of Clusters

The clusters selected according to the automated procedures outlined above were classified using the Viterbi algorithm (Forney, 1973; Chung et al., 1990; program DETECT). Briefly, a bare Markov model, having only one state for each conductance class, was used to describe the currents within clusters. The Viterbi al-

gorithm is a computationally efficient method of estimating the most likely state sequence through a series of current samples, based on both amplitude and kinetic criteria. Each model had one main level, one sublevel, and one fully closed level. Each level had additive noise (uncorrelated, Gaussian) of a variance that could differ from state to state. Each current sample was associated with a state of the model according to both amplitude and transition probabilities, and a log likelihood (LL) of the optimal state sequence was obtained. For each cluster, such an LL was computed using different models, and the cluster was classified according to the model that produced the highest LL. We emphasize that this classification procedure did not involve any optimization because all of the parameters of the model were fixed.

The number of models applied to each current record was determined by inspection of the clusters. In addition to individual clusters, we examined the number of patterns from homogeneous patches where one pattern predominated (see Figs. 3 and 6), and the number of groups that were apparent in scatter plots of main/sub amplitudes of all valid clusters in patches, regardless of their classification by pattern (see Figs. 5 and 10).

For the NR1 hybrid experiments, six different models were applied to each cluster. The current amplitudes of the six models were (see Fig. 6; inward currents in pA, main/sub): 7.7/5.2, 7.7/5.2, 6.7/4.7, 5.4/3.7, 4.4/ 3.1, and 4.6/2.4. In all patterns but one, the kinetic scheme was:

$$\begin{array}{ccc} 1000 & 500 \\ \text{closed} \leftrightarrow \text{sub} \leftrightarrow \text{main} \\ 100 & 500 \end{array} \qquad \text{(Model 1)}$$

where the rate constants have the units s^{-1}. The lone exception pertained to the second pattern (H1), where $k_{sub \to main}$ was $150 \ s^{-1}$ and $k_{main \to sub}$ was $850 \ s^{-1}$. The LL is mainly determined by cluster amplitudes rather than interval durations and, with the exception of the Q/Q and H1 patterns, cluster classification was not sensitive to either the connectivity or rate constants of the model. For the NR2 hybrids experiments, three models were applied to each cluster, with rate constants as in Model 1 and amplitudes (main/sub, in pA) of 7.7/5.2, 7.3/3.2, and 6.1/0.8. In all of the models the standard deviation of the additive noise was 0.5 pA. To allow for missed events, all states of the model were allowed to interconvert with a probability $>10^{-5}$.

Clusters were classified according to the model that produced the highest LL. There were two exceptions to this classification procedure. First, if the likelihood of the best model was not above a minimal standard, the cluster in question was considered to be invalid (i.e., not belonging to any of the tested models) and was rejected from further analysis. For a homogeneous population of Q/Q clusters (from a pure subunit injection experiment), the LL/ms according to the Q/Q model was 6.85 ± 0.93 ($n = 76$). Homogeneous populations of clusters (after separation) produced an LL/ms of $\sim 6 \pm 1$ for the optimal model (see the last row of Tables II and III). From these considerations, a value 10 LL U/ms was selected as the standard for rejection.

For every patch, each of the reject clusters was examined by eye because a low LL might indicate the presence of a new pattern; i.e., a cluster that did not correspond to any of the tested models. However, this was not the case. For all rejected clusters, the low LL could be attributed to errors in the baseline estimate, a chance juxtaposition of different current patterns in one cluster, overlapping currents, seal breakdown, current spikes, and/or other noise sources (see Fig. 8, *bottom right*). Thus, the visual check confirmed that clusters that were rejected on the absolute LL criterion did not arise from a novel pattern of receptor currents.

The second exception to classification by LL was that clusters in which the occupancy probability of either the main or sublevel was zero (i.e., clusters with no submain transitions) were rejected from the analysis because the main level of some patterns was similar to the sublevels of others, making the classification of these clusters ambiguous. For example, a cluster with a single opening of -4.6 pA could be associated either with a main level sojourn of an N/Q or a sublevel sojourn of an H2 receptor. Typically, $< \sim 10\%$ of clusters were rejected for either of these two reasons.

There was considerable scatter in the number of selected clusters per patch (range: 9–461) because of patch-to-patch variations in the duration of the recording, the number of channels, and, perhaps, the activation parameters of receptors. On average, ~ 60 clusters were analyzed per patch. In experiments with pure wild-type and mutant subunits, 50 patches were examined (Table I), and 299 clusters were isolated from eight patches. In experiments where a mixture of wild-type and mutant NR2 subunits were examined, 693 clusters were isolated from 13 patches. In experiments where a mixture of wild-type and mutant NR1 subunits were examined, 2,879 clusters were isolated from 44 patches.

Pattern Characteristics

Once clusters had been separated according to pattern, the amplitudes, standard deviations, interval durations, and occupancy probabilities of the closed, sub-, and main current levels of clusters were determined using a hidden Markov model method known as the segmentation k-means algorithm (program SKM; Qin et al., 1996*b*; see Juang and Rabiner, 1990). This is an optimization method that computes the most likely state sequence using the Viterbi algorithm, and then re-estimates model parameters to achieve the maximum likelihood of this state sequence. The optimized parameters are shown in Tables II and III. In receptors comprised of purely wild-type NR1 and purely mutant NR2 subunits (Q/N receptors), the sublevel was not readily distinguished from the baseline in the cluster-based analyses, so that in these experiments the results were different from those estimated by applying SKM to the entire record (Table I).

The kinetic scheme had three conductance states (closed, sub, main). In the SKM method, transitions between all states are allowed; i.e., the three conductance states were fully interconnected. The starting values for the mean amplitudes and standard deviations of each state were determined by interactively selecting segments of the current that appeared to correspond to each state of the model. This selection was done only for the first cluster in the patch record; the same starting values were applied to all of the remaining clusters. The starting rate constants were all $1,000 \ s^{-1}$. From these initial estimates, the most likely state sequence through the cluster was calculated using the Viterbi algorithm. Model parameters (amplitudes, variances, and transition probabilities) were then re-estimated from the state sequence, and a new most likely state sequence was computed. This procedure was repeated iteratively until convergence, defined by both a small change in the log likelihood (<0.01 likelihood units) and a small average derivative of the model parameters (<0.01). Typically, the model parameters converged in less than five iterations. The procedure was repeated for all clusters. The outputs of interest from the SKM algorithm were a model that encodes the mean amplitude, noise standard deviation, mean lifetime, and occupancy probability for each current level, and the likelihood of the optimal state sequence through the current.

R E S U L T S

Receptors Composed of Pure Mutant or Wild-Type Subunits

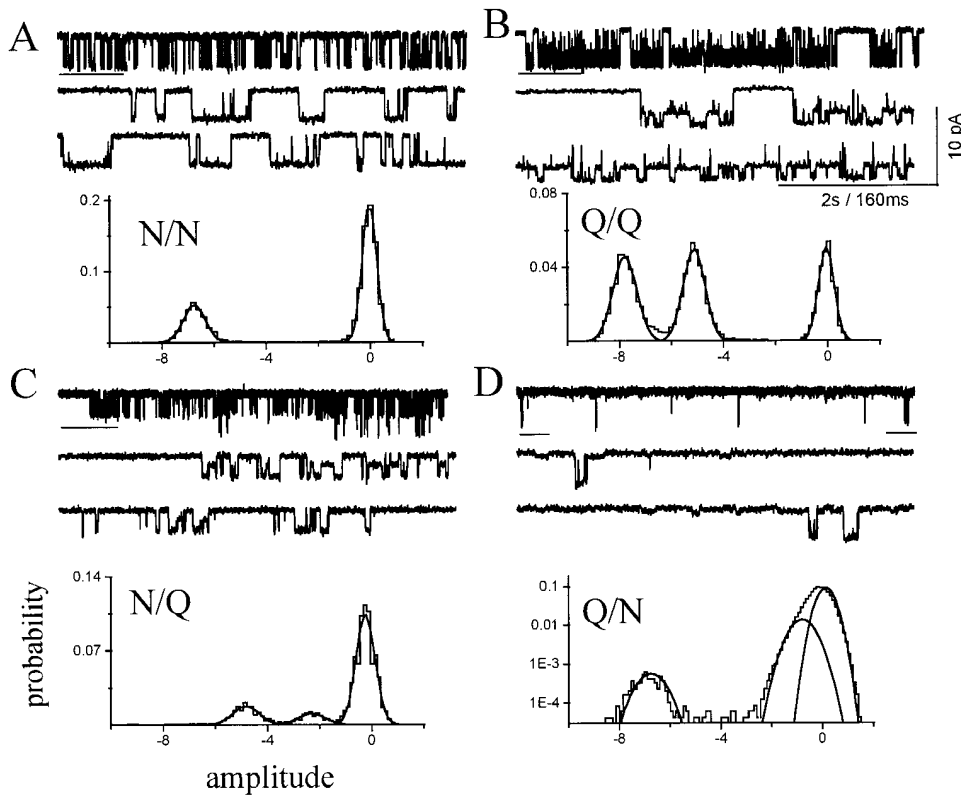We first examined single-channel currents in oocytes injected with NR1 and NR2B subunits that had purely

FIGURE 1. Pure wild-type (*N*) or mutant (*Q*) subunits for both NR1 and NR2B subunits produce channels with distinct current patterns. For each panel, low and high time resolution displays of the current, the injection protocol (NR1/NR2B), and an all-point amplitude histogram for the continuous record are shown. Outside-out patches were superfused with 50 μM NMDA plus 10 μM glycine in divalent-cation free solution. The properties of the currents (−80 mV) are detailed in Table I. The underlined region of the low time resolution trace is shown at an expanded time scale; all traces are continuous. (*A*) Injection of wild-type NR1 and NR2B subunit RNAs produces channels with a single open channel current level of −6.7 pA. (*B*) Injection of mutant NR1 and NR2B subunits produces channels that have a main level of −7.7 pA and a sublevel of −5.0 pA, each of which is occupied with approximately equal probability. (*C*) Injection of wild-type NR1 and mutant NR2B subunits produces channels that have a main level of −4.5 pA and a sublevel of −2.1 pA. The main level is occupied with a slightly higher probability. (*D*) Injection of mutant NR1 and wild-type NR2B subunits produces channels that have a main level of −6.1 and a sublevel of −0.9 pA. The probability of residing in the larger current level is relatively small. For clarity, the y-axis is logarithmic in this panel only.

wild-type (N) or mutant (Q) residues at the N_0 position. In these experiments, it is expected that four compositions of receptor would form: N/N, Q/Q, N/Q, and Q/N, where the letters N and Q refer to the N_0 residue of the NR1/NR2B subunit. With injection of pure subunits, we could study receptors in which the type (N or Q) of subunit was unambiguous, but the copy number and position of the subunits was unknown.

Fig. 1 shows continuous current records from patches expressing each of the four combinations of pure subunits. When open, N/N (wild-type) receptors occupy a main current level with a probability near 1.0. At −80 mV, the amplitude of this level is −6.7 pA. In the presence of 1 mM Ca^{2+}, subconductance states are present in rat wild-type NR (Stern et al., 1992), but in Ca^{+2}-free solutions subconductance states are virtually nonexistent in mouse NR (Premkumar and Auerbach, 1996*a*). Q/Q receptors occupy a main (−7.7 pA) and a sub- (−5.1 pA) level with approximately equal probability. N/Q receptors also exhibit both a main (−4.5 pA) and a sub- (−2.1 pA) level, with the former occupied with a higher probability. Q/N receptors give rise

TABLE I

Single-Channel Parameters for Receptors Composed of Pure Wild-Type and Mutant Subunits

		N/N	Q/Q	N/Q	Q/N
	Patches	18	17	9	6
Amplitude (pA)	i_{main}	−6.73 ± 0.24	−7.68 ± 0.24	−4.49 ± 0.22	−6.12 ± 0.5
	i_{sub}	—	−5.05 ± 0.22	−2.08 ± 0.32	−0.89 ± 0.12
Relative occupancy	$P_{rel, main}$	1	0.48 ± 0.07	0.67 ± 0.05	0.10 ± 0.06
	$P_{rel, sub}$	0	0.52 ± 0.07	0.33 ± 0.05	0.90 ± 0.06

Oocytes were injected with purely wild-type (N) or purely mutant (Q) subunits. The receptor composition is given as NR1/NR2. i_{main} is the main level current amplitude (pA), and i_{sub} is the sublevel current amplitude. P_{rel} is the relative probability of occupying the current level given that the channel was not closed. The values were estimated from continuous current recordings; i.e., without isolation of clusters. Values are mean ± SD. Note that the relative occupancy probabilities calculated from continuous records are not the same as the cluster occupancy probabilities reported in Tables II and III as these also include closed sojourns within clusters.
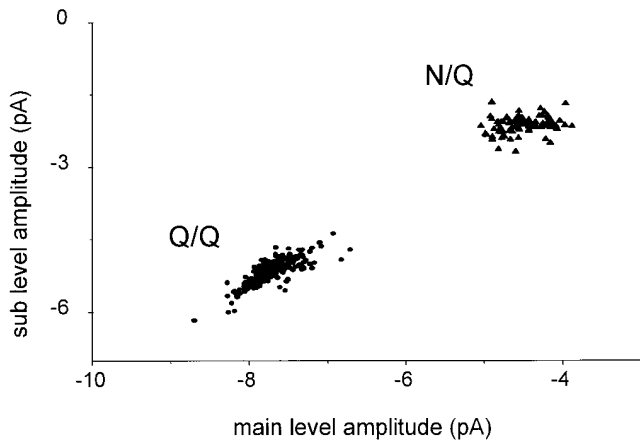
FIGURE 2. Cluster sub- versus main level amplitudes for Q/Q and N/Q receptor compositions. Oocytes were injected with either mutant NR1 plus mutant NR2 (Q/Q receptors; ●, five patches), or wild-type NR1 plus mutant NR2 (N/Q receptors; ▲, three patches). All valid clusters in all of the patches are plotted. A single pattern of current is present with these injections of unmixed subunits. The diagonal distribution of Q/Q amplitudes indicates that scatter in the main and sublevels is correlated.

and N/Q patterns. There is substantial scatter in the amplitudes, mostly from patch-to-patch. For the Q/Q clusters (5 patches, 207 clusters; mean ± SD), the main level amplitude was −7.73 ± 0.29 pA, and ranged from −8.7 to −6.7 pA. For the N/Q clusters (2 patches, 97 clusters), the main amplitude was −4.49 ± 0.28 pA, and ranged from −5.0 to −3.9 pA.

The extent of the scatter in amplitudes is significant and limited the accuracy of the separation of current patterns. The sources of the scatter were not investigated, but might include small variations in the membrane potential, differences in the local receptor environment in the outside-out patches (e.g., interactions with the cytoskeleton; Clark et. al., 1997), and/or variations in posttranslational processing (e.g., phosphorylation or glycosylation) of receptor subunits. The continuous (as opposed to modal) nature of the scatter suggests that receptors assembled from pure subunits indeed produce a single current pattern. The ratio of sub-/main level amplitudes (0.66 ± 0.02 for Q/Q) was more consistent than either amplitude alone, indicating that the sources of variance influence both current levels approximately equally.

Patterns of Receptors Composed of a Mixture of Mutant and Wild-Type NR2 Subunits

To ascertain the number of copies of the NR2B subunit per receptor, mixtures of wild-type and mutant NR2B subunits were expressed. The mixture pertained only to the NR2 subunit; in these experiments, the NR1 subunit was purely mutant at the N_0 position.

Three current patterns were apparent in these experiments. In most of the patches, only one of these three

to a main level (−6.2 pA), and a long lived, low amplitude (−0.9 pA) sublevel. For each composition, the amplitude and relative occupancy probability of each current level is given in Table I.

Upon injection of pure N or Q subunits, only one current pattern was observed for each of the four receptor compositions. Clusters of opening were isolated by an automated procedure (i.e., without selection by eye). Fig. 2 shows a plot of the sub- versus main amplitudes, compiled on a cluster-by-cluster basis, for the Q/Q
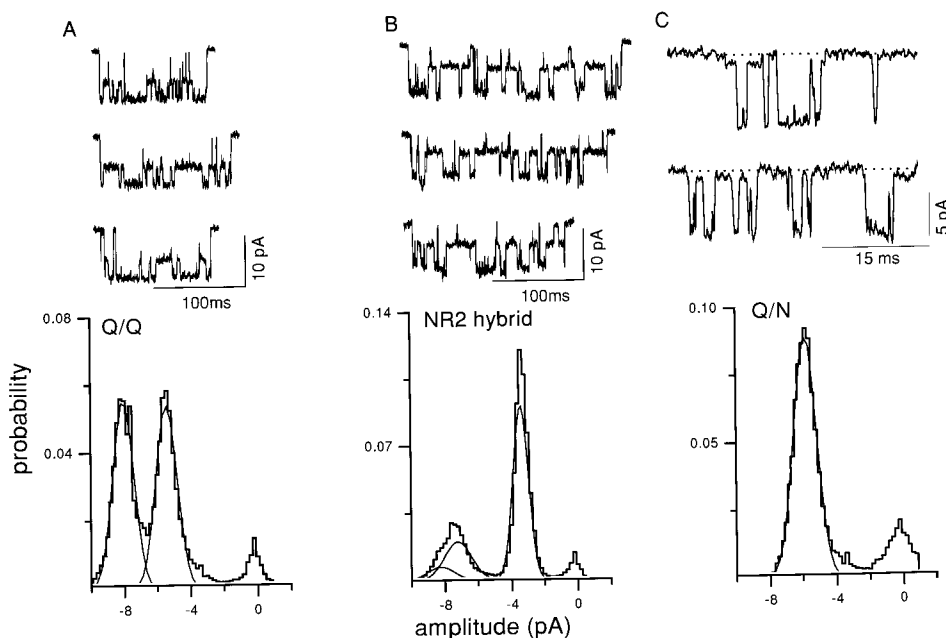

FIGURE 3. Three cluster patterns are produced upon expression of a mixture of NR2 plus mutant NR1 subunits. Each panel shows example clusters and the amplitude histogram of all clusters from a single patch. (*A*) The Q/Q pattern (main = −8.0 pA, sub = −5.4 pA; see Fig. 1 *B*). (*B*) A novel pattern (NR2 hybrid) with three open channel levels (−8.3, −7.0, and −3.4 pA). This pattern was never observed in receptors with purely mutant or wild-type subunits and, therefore, arises from a hybrid receptor that has both N and Q NR2B subunits. (*C*) The Q/N pattern (main = −5.9 pA, sub = −0.8 pA; see Fig. 1 *D*). To show the sublevel more clearly, a dashed line marks the baseline, and the example traces showing of this pattern were taken from continuous recordings.

Single-Channel Parameters for Receptors Composed of Pure Mutant NR1 Subunits, and a Mixture of Wild-Type or Mutant NR2 Subunits

Pattern		Q/Q	hybrid	Q/N
	Patches	2	12	3
Amplitude (pA)	i_{main}	-7.83 ± 0.27	-8.03 ± 0.42	-6.03 ± 0.18
	i_{sub1}	—	-6.74 ± 0.32	—
	i_{sub2}	-5.10 ± 0.25	-3.19 ± 0.21	-0.75 ± 0.12
	i_{closed}	-0.29 ± 0.43	-0.34 ± 0.27	-0.03 ± 0.05
rms noise(pA)	SD_{main}	0.60 ± 0.16	0.53 ± 0.14	0.79 ± 0.08
	SD_{sub1}	—	0.76 ± 0.18	—
	SD_{sub2}	0.66 ± 0.16	0.42 ± 0.07	0.45 ± 0.13
	SD_{closed}	0.45 ± 0.32	0.50 ± 0.17	0.23 ± 0.30
Occupancy	P_{main}	0.42 ± 0.13	0.12 ± 0.09	—
	P_{sub1}	—	0.21 ± 0.10	—
	P_{sub2}	0.49 ± 0.14	0.59 ± 0.08	—
	P_{closed}	0.08 ± 0.09	0.08 ± 0.07	—
Lifetime (ms)	τ_{main}	2.75 ± 1.04	3.94 ± 2.42	5.68 ± 1.90
	τ_{sub1}	—	1.97 ± 0.88	—
	τ_{sub2}	2.88 ± 1.42	5.06 ± 2.23	1.11 ± 0.64
	τ_{closed}	1.43 ± 1.35	0.99 ± 0.58	0.54 ± 0.68
$-LL/ms$		5.90 ± 0.75	4.85 ± 0.80	3.75 ± 0.60

Oocytes were injected with pure Q NR1 subunits and a mixture of N and Q NR2 subunits. All values pertain only to clusters and were estimated using the SKM algorithm (see METHODS). i is the mean amplitude (pA), SD is the noise standard deviation (pA^2), P is the probability of occupying a current level within a cluster, τ is the mean lifetime (ms), and LL is the log likelihood. Patches are the number of patches in which a pattern was observed. Values are mean ± SD. No occupancy probabilities are given for the Q/N pattern because, due to the small current of the sublevel and limitations of the procedure employed to extract clusters from the data, long duration openings to the sublevel were excluded.

patterns was present in a patch. Examples are shown in Fig. 3, in which clusters, and amplitude histograms of all clusters, are displayed. One pattern was identical to that observed when pure Q NR2 subunits were expressed, and could thus be identified as arising from Q/Q receptors (Fig. 3 *A*). Another pattern was identical to that of pure Q/N receptors (Fig. 3 *C*). The third current pattern was novel and had three open channel current levels (see Fig. 3 *B, middle trace*). This pattern was never observed in injections of pure mutant or wild-type subunits, and we therefore conclude that this pattern arises from hybrid receptors composed of both mutant and wild-type NR2B subunits. In the hybrid pattern, three open channel currents are apparent, with mean amplitudes of -8.0, -6.7, and -3.2 pA (Table II). Note that in the all-points amplitude histogram of the NR2 hybrid (Fig. 3 *B*), the two largest amplitude levels merge into a single, broad peak.

In some patches, more than one current pattern was apparent. Fig. 4 shows an example in which clusters with the Q/Q or the hybrid pattern were both present in a single patch. The amplitude histogram of all the clusters in this patch shows three open channel peaks plus one baseline peak (Fig. 4 *A*). The peak at ~-7.5 pA in the all-point histogram reflects the sum of the activity of both receptor compositions because the main amplitudes of the Q/Q and hybrid patterns are similar. Clusters were separated into homogeneous groups ac-

cording to pattern using a log likelihood method. The amplitude histograms of the separated groups are also shown in Fig. 4 *B*. In this patch, there were 104 Q/Q clusters and 25 hybrid clusters.

Fig. 5 shows a scatter plot of the main versus sublevel amplitudes for all clusters from 10 representative patches from oocytes injected with a 1:1 mixture of N and Q NR2 subunits. Three groups are apparent, corresponding to the Q/Q, NR2 hybrid, and Q/N receptor compositions. Note that the mean and variance of the Q/Q pattern from the mixed injection is similar to that of the pure Q/Q receptors (Fig. 2). The number of clusters of each subtype does not accurately reflect the number of receptors of each composition. In particular, Q/N receptors are relatively rare in the cluster-based analysis because in the automated procedure the sublevel was often not differentiated from the fully closed channel.

The amplitude, noise standard deviations, lifetimes, and current level occupancies of the subtypes of receptors expressed when a mixture of wild-type and mutant NR2 subunits was injected is given in Table II. In the hybrid receptors, the two highest open channel amplitudes differ by ~1.3 pA (or 16 pS, assuming a reversal potential of 0 mV), while the sublevel (-3.2 pA) was approximately the average of the Q/Q and Q/N sublevels.

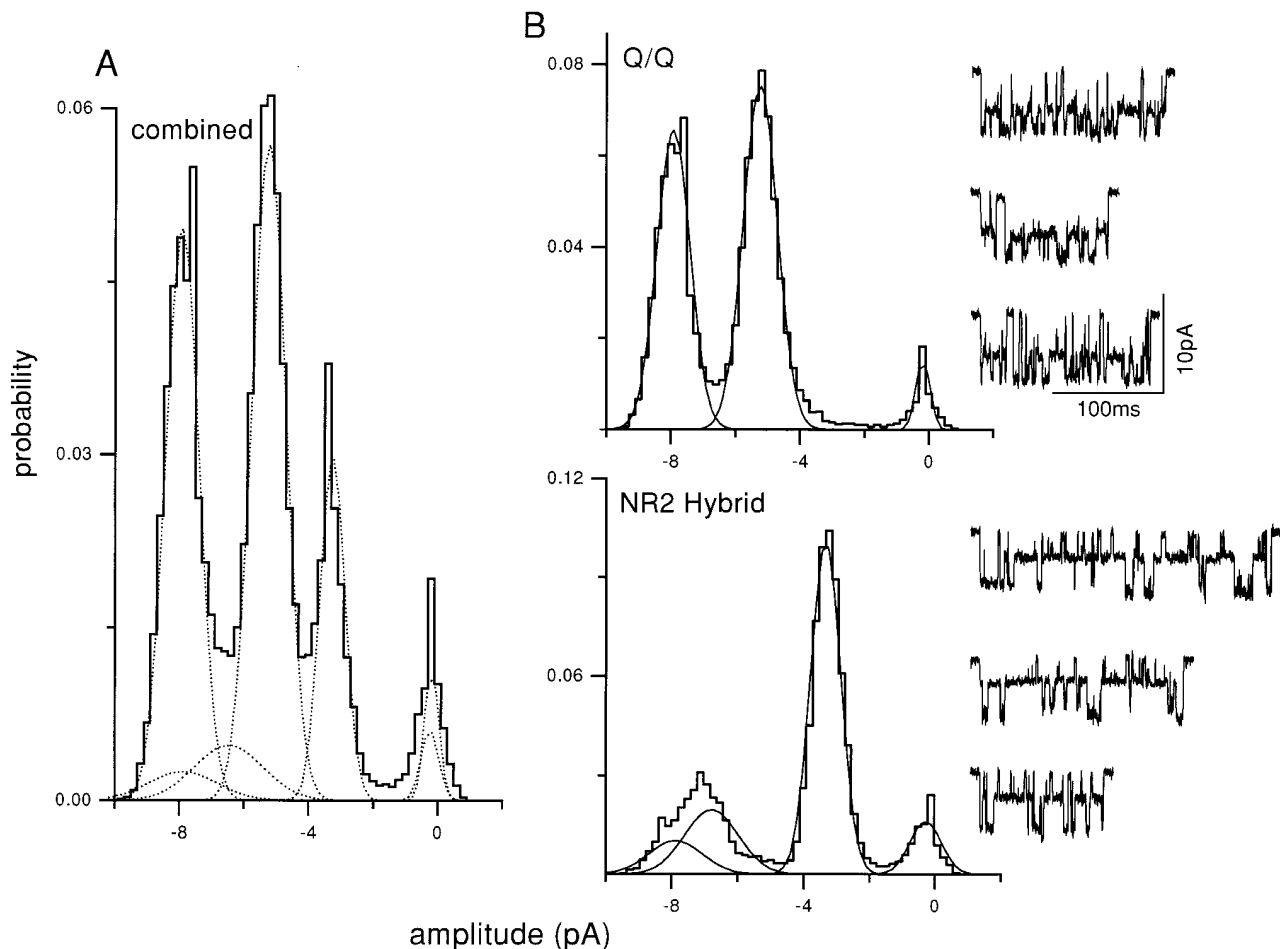To summarize, three current patterns are produced

FIGURE 4. Separation of clusters by pattern: mixed NR2 subunit expression. The oocyte was injected with pure mutant NR1 subunits, plus a 1:1 mixture of wild-type and mutant NR2 subunits. Clusters with the Q/Q and NR2 hybrid patterns were apparent, and were separated using a log likelihood criterion. (*A*) All-points amplitude histogram of all 134 clusters in the patch, before separation. (*B*) Amplitude histograms of clusters, after separation. (*top*) Histogram and examples of separated Q/Q clusters ($n = 100$, main $= -7.9$ pA, sub $= -5.2$ pA); (*bottom*) histogram and examples of NR2 hybrid clusters ($n = 25$, open channel amplitudes of -7.9, -6.6, and -3.1 pA). 10 clusters (7.5%) were rejected because of a low log likelihood (not shown). When summed, the Gaussian components of the separated histograms (dotted lines in *A*) plus that of the rejected clusters equal the combined histogram.

when a mixture of N and Q NR2 subunits are expressed.

Patterns from Receptors Composed of a Mixture of Mutant and Wild-Type NR1 Subunits

To deduce the number of copies of the NR1 subunit per receptor, mixtures of wild type (N) and mutant (Q) NR1 subunits were expressed. The mixture pertained only to the NR1 subunit, as the NR2 subunit was purely mutant.

Several current patterns were observed in these experiments. Usually more than one current pattern was present in a patch. In some patches, however, a single current pattern predominated, and the amplitude histograms could be described by the sum of only three Gaussian components (corresponding to the main,

sub-, and closed levels). Examples of clusters, and amplitude histograms from such patches, are shown in Fig. 6.

From the all-point amplitude histograms of these patches, six current patterns could be identified. Two of the patterns were identical to receptors expressed with pure subunits and could therefore be identified as corresponding to the Q/Q (Fig. 6 *A*) and N/Q patterns (Fig. 6 *F*). In addition, four novel current patterns were apparent, called H1–H4. Since injections of purely N or Q NR1 subunits result in a single pattern (Fig. 1, *A* and *C*), the novel patterns presumably arise from hybrid receptors composed of both N and Q NR1 subunits.

Although some patches appeared to be nearly homogeneous with regard to the pattern of clusters, usually multiple cluster patterns were present in a single patch.
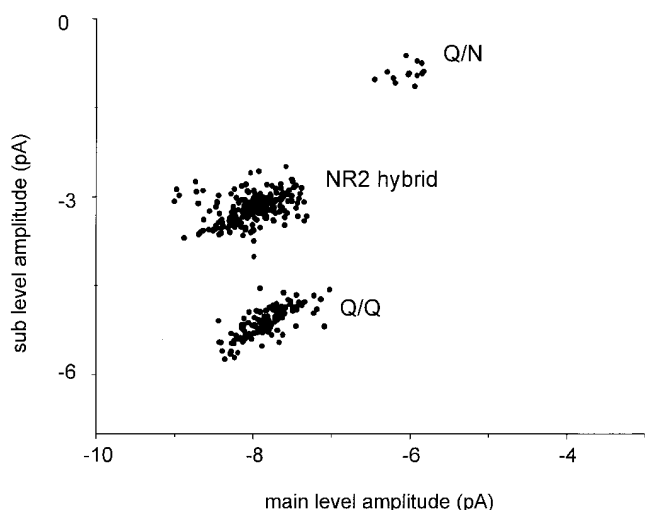
FIGURE 5. Cluster sub- versus main level amplitudes for mixed NR2 subunit expression. Oocytes were injected with a mixture of wild-type and mutant NR2, plus pure mutant NR1 subunit RNAs. All valid clusters from 10 patches are plotted, irrespective of their classification according to pattern. Three groups are apparent. The bottom group is Q/Q receptors (see Fig. 2). The central group is NR2 hybrid receptors, composed of both wild-type and mutant NR2 subunits. There are three open channel current levels in this pattern; here, the smallest amplitude is plotted as a function of the

In these cases, peaks of the all-point amplitude histogram often could not be directly associated with a current level of a specific pattern. First, the Q/Q and H1 patterns have similar amplitudes and are distinguished only on the basis of the sublevel occupancy probability. Second, the main levels of some patterns (N/Q: −4.6 pA; H3: −5.4 pA) are similar to the sublevels of others (H2: −4.7 pA; Q/Q and H1: −5.3 pA) and current from each level cannot be resolved as separate peaks. Thus, the number of clusters of each pattern could not, in general, be estimated from fitting amplitude histograms, and clusters were instead classified as belonging to the Q/Q, N/Q, or one of the hybrid patterns using the log likelihood as a discriminator.

In the patch shown in Fig. 7, only two types of clusters were apparent. The amplitude histogram of all clusters shows a continuous spread of current between ~−8 and −4 pA (Fig. 7 A). Upon separation, 39% of clusters were associated with the H1 pattern, 58% with the H2 pattern, and 3% of clusters could not be associ-

largest amplitude. The top group is Q/N receptors. The number of clusters in this group is relatively small because during the automated analysis of clusters the sublevel was often not detected.
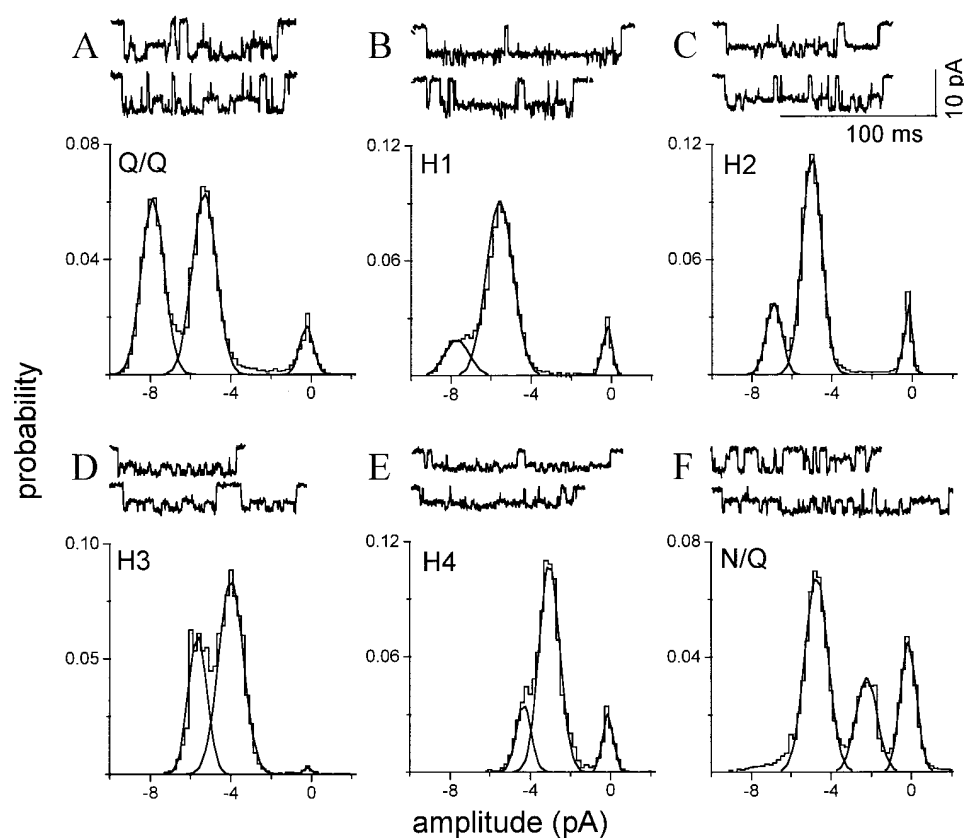

FIGURE 6. Six homogeneous cluster patterns are apparent upon expression of a mixture of NR1 plus mutant NR2 subunits. Each panel is from one patch in which one pattern predominated. The amplitude histograms pertain to all clusters in the patch; i.e., with no separation according to pattern. (A) The Q/Q pattern (see Fig. 1 B; n = 98 clusters). (B) Hybrid receptor pattern H1, with a main and sublevel similar to the Q/Q pattern but with a much higher relative occupancy in the sublevel (n = 44 clusters). (C) Hybrid receptor pattern H2, with a main level amplitude ~15% lower than the Q/Q main level and with a preferential occupancy of the sublevel (n = 110 clusters). (D) Hybrid receptor pattern H3, with a main level amplitude ~30% lower than the Q/Q main level, and nearly equal main and sublevel occupancies (n = 14 clusters). (E) Hybrid receptor pattern H4, with a main level of ~40% lower than the Q/Q pattern, and a preferential occupancy of the sublevel (n = 13 clusters). (F) The N/Q pattern (see Fig. 1 C; n = 165 clusters). The amplitude, standard deviation, occupancy, and lifetime of the main and sublevel of each of these patterns is given in Table III.
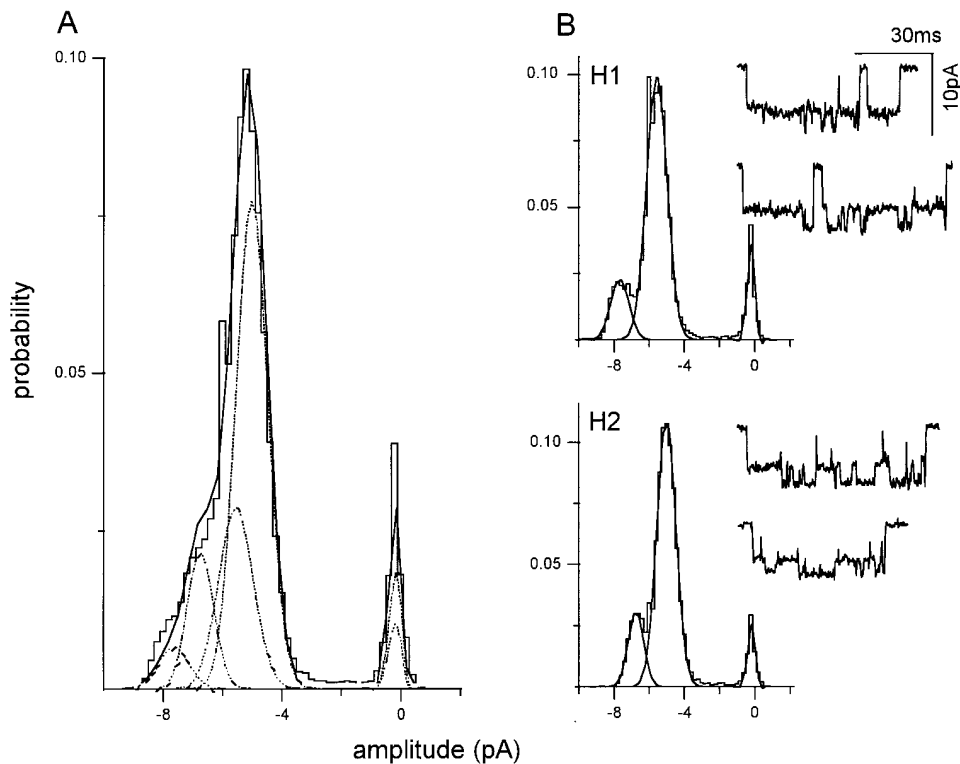
FIGURE 7. Separation of clusters by pattern: a mixed NR1 subunit patch with two patterns. The oocyte was injected with a 1:1 mixture of wild-type and mutant NR1 subunits, plus pure mutant NR2 subunits. Clusters with the H1 and H2 patterns were apparent, and were separated using a log likelihood criterion. (*A*) Amplitude histogram of all 94 clusters in the patch, before separation. (*B*) Amplitude histograms of clusters after separation. (*top*) H1 clusters ($n = 38$; main = -7.8 pA, sub = -5.6 pA; see Fig. 6 *B*). (*bottom*) H2 clusters ($n = 56$; main = -6.8 pA, sub = -4.9 pA; see Fig. 6 *C*). Three clusters were rejected because of a low likelihood (not shown). When summed, the Gaussian components of the separated histograms (*A, dotted lines*) plus the rejected clusters equals the combined histogram. For examples of homogeneous H1 and H2 patterns see Fig. 6.

ated with any of the six patterns that were tested. Examination of each of these rejected clusters showed that the low LL arose from either noise, channel overlap (multiples), or the chance juxtaposition of an H1 and an H2 cluster. The separation procedure successfully decomposed the global all-points histogram into its components (Fig. 7 *B*).

Fig. 8 shows a patch in which three cluster patterns were present. In this example, all 25 clusters that were present in this patch are shown, along with their associated amplitude histograms after decomposition by pattern. The H1 amplitude histogram is similar to those shown for H1 clusters in other patches (Figs. 6 and 7).

Fig. 9 shows a more complicated patch in which four current patterns were apparent. A continuous stretch of current is shown in Fig. 9 *A*, and the global amplitude histogram of all 444 clusters in this patch is shown in Fig 9 *B*. After separation, H1, H3, H4, and N/Q clusters were identified. Note that for the examples shown in Figs. 6–9, the amplitude histograms for each receptor subtype were similar between patches, supporting the conclusion that the current patterns are modal, as opposed to continuous, in nature.

In Fig. 10, main and sublevel amplitudes are shown for all valid clusters recorded in 10 patches obtained after injecting a mixture of mutant and wild-type NR1 subunits. Despite substantial scatter, five distinct groups can be distinguished, with main and sublevel amplitudes that correspond to the patterns identified

in the homogeneous and separated patches. In these data, all of the current patterns that were previously identified were present, and no additional cluster patterns were observed. Recall that the Q/Q and H1 patterns have similar amplitudes and form a single group (*bottom left*) in the scatter plot. Evidence that the Q/Q and H1 patterns arise from distinct populations of receptors is provided in the next section.

The amplitude and occupancy parameters for the Q/Q, H1–H4, and N/Q patterns obtained from oocytes injected with a mixture of N and Q NR1 subunits are summarized in Table III. The ratio of the main/sublevel amplitude is ~1.4 for the Q/Q and all of the hybrid patterns, and ~2.1 for the N/Q pattern. Since some of the hybrid patterns presumably reflect receptors having different numbers of N and Q NR1 subunits, this result indicates that the number of mutant subunits at the NR1 N_0 position does not uniquely determine the relative currents of the main and sublevels. The main amplitude changes in a consistent manner between hybrids, decreasing by ~1.2 pA (~15 pS) between H1–H2, H2–H3, and H3–H4. The sublevels of the H1 and H2 patterns were preferentially occupied with a much greater probability ($P = 0.85$ and 0.70, respectively), while the main and sublevels of the H3 and H4 patterns were occupied with approximately equal probability.

Fig. 11 shows the time dependence of the cluster frequency and current amplitudes in a patch with four dif-
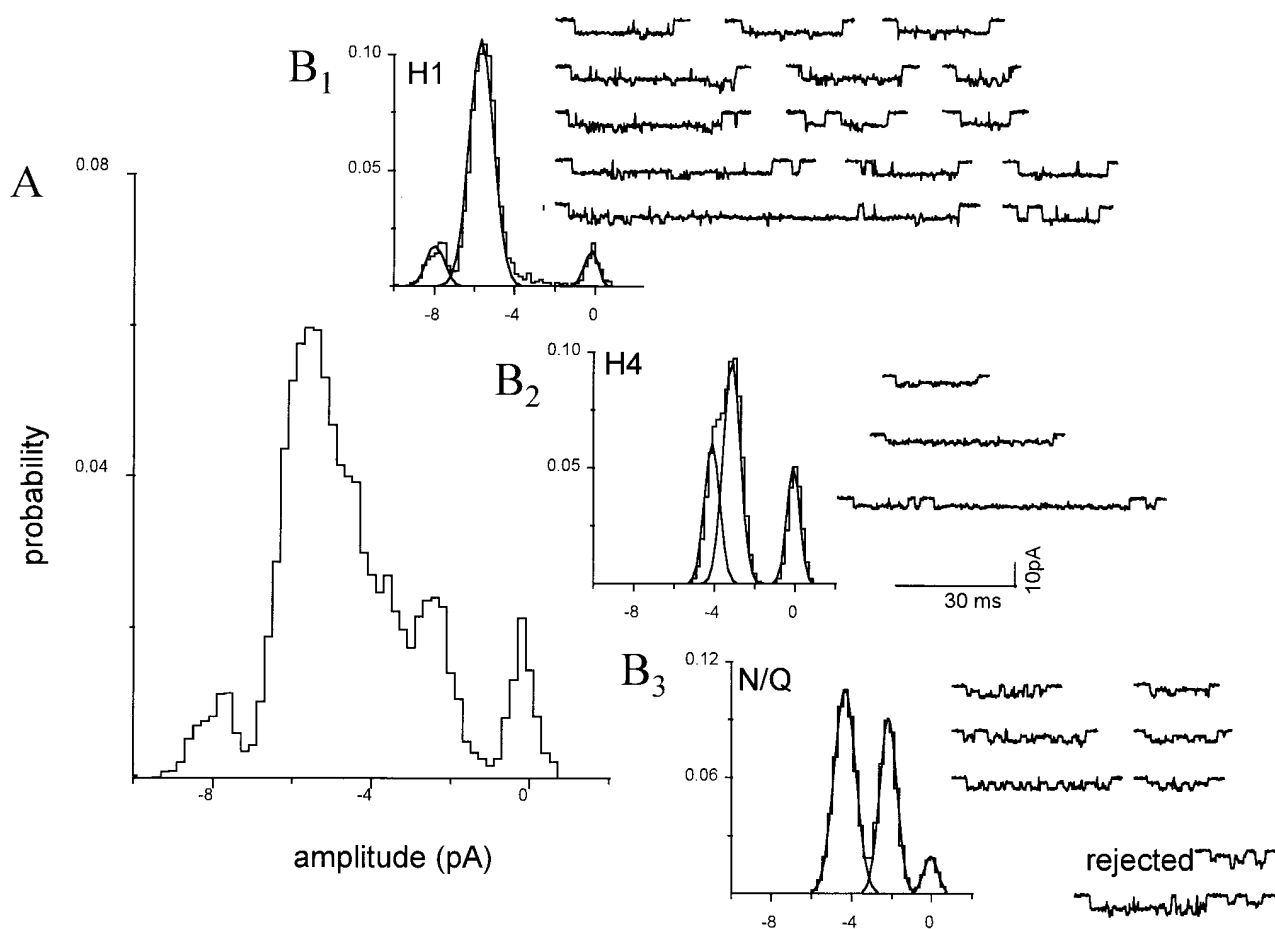
FIGURE 8. Separation of clusters by pattern: a mixed NR1 subunit patch with three patterns. The oocyte was injected with a 1:1 mixture of wild-type and mutant NR1 subunits plus pure mutant NR2 subunits. Clusters with the H1, H3, and H4 patterns were apparent, and were separated using a log likelihood criterion. All 25 clusters in this patch are shown. (*A*) Amplitude histogram of all clusters, before separation. Only the closed channel component (*rightmost*) is a distinct peak. (*B*) Amplitude histograms of clusters after separation by pattern. (*B, 1*) H1 clusters ($n = 14$). (*B, 2*) H4 clusters ($n = 3$). (*B, 3*) N/Q clusters ($n = 6$). (*bottom right*) Rejected clusters ($n = 2$) that had a low likelihood because of a multiple opening, or the chance juxtaposition of an H1 and an N/Q cluster. For examples of homogeneous H1, H4, and N/Q patterns see Fig. 6.

ferent cluster patterns. Over a 4-min period, there was no drift in the main and sublevel amplitudes within each pattern, and no obvious correlation in the frequencies of occurrence of different patterns. This result is consistent with the presence of four distinct, stable populations of receptor in the patch.

To summarize, six current patterns are produced when a mixture of N and Q NR1 subunits are expressed.

Separation of the Q/Q and H1 Patterns

Fig. 12 shows that receptors exhibiting the Q/Q and H1 patterns are differentially sensitive to external Ca^{2+}. Previous work has shown that low ($\sim$5 μM) concentrations of Ca^{2+} specifically block the sublevel of pure Q/Q receptors (Premkumar and Auerbach, 1996*a*). In the patch shown in Fig. 12, in Ca^{2+}-free solutions (at a membrane potential of -160 mV), only the Q/Q and

H1 patterns were present. At this voltage, the main level amplitude is -12.8 pA and the sublevel amplitude is -9.2 pA (Fig. 12 *A*). The relative frequency of each pattern was approximately equal. After the addition of 16.7 μM Ca^{2+} to the extracellular solution, two new patterns having distinct main and sublevel amplitudes were apparent. One of the current patterns was that expected from Ca^{2+}-blocked Q/Q receptors, in which the main level was -12.2 pA and the sublevel was -2.4 pA. The other current pattern was novel and had a main level of -10.2 pA and a sublevel of -3.4 pA (Fig. 12 *B*). Fitting the all-points histogram to the sum of five Gaussian components indicated that the relative frequency of each pattern was approximately equal. We conclude that this novel pattern arises from H1 receptors in the patch, and the Ca^{2+} block of the H1 receptor sublevel is less than that of Q/Q receptors. This result unequivocally shows that the Q/Q and H1 patterns do not reflect

A

B

C

H1

H3

H4

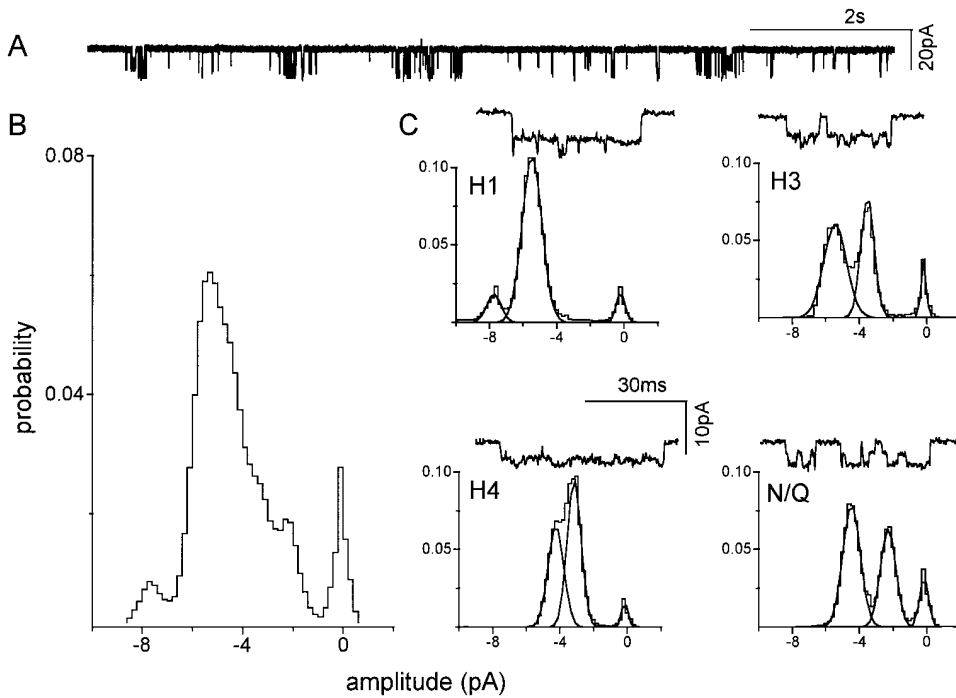N/Q

2s
20pA

30ms
10pA

probability

amplitude (pA)

FIGURE 9. Separation of clusters by pattern: a mixed NR1 subunit patch with four patterns. The oocyte was injected with a 1:1 mixture of wild-type and mutant NR1 subunits, plus pure mutant NR2 subunits, and the outside-out patch was superfused with 20 μM NMDA plus pure 10-μM glycine in divalent-cation-free solution. Clusters with the H1, H3, H4, and N/Q patterns were apparent and were separated using a log likelihood criterion. (*A*) Continuous 10-s trace at low time resolution. (*B*) Amplitude histogram from all 444 clusters in the patch, before separation. Only the baseline, and a component at -7.8 pA, are distinct peaks. (*C*) Amplitude histograms of clusters after separation by pattern. (*top left*) H1 clusters ($n = 154$), (*top right*) H3 clusters ($n = 48$), (*bottom left*) H4 clusters ($n = 34$), (*bottom right*) N/Q clusters ($n = 164$). Rejected clusters ($n = 44$) are not shown. For examples of homogeneous H1, H3, H4, and N/Q patterns see Fig. 6.

a continuum of kinetic behaviors, but rather arise from different populations of receptors.

Counting Cluster Patterns as a Function of the Q:N Injection Ratio

Separation of clusters according to pattern according to the maximum LL value was carried out for 64

patches. Of these, 6 were from pure subunit injections, 43 were from NR1 mixtures, and 15 were from NR2 mixtures. The pure injections were included as a test of the accuracy of the separation procedure, because in these patches a single pattern of clusters was expected (Q/Q or N/Q). In the pure Q/Q injection experiments, of the 212 clusters that were present, 195 were classified as Q/Q, 11 as H1, and 6 as H2. In the pure

N/Q

H4

H3

Q/Q and H1

H2

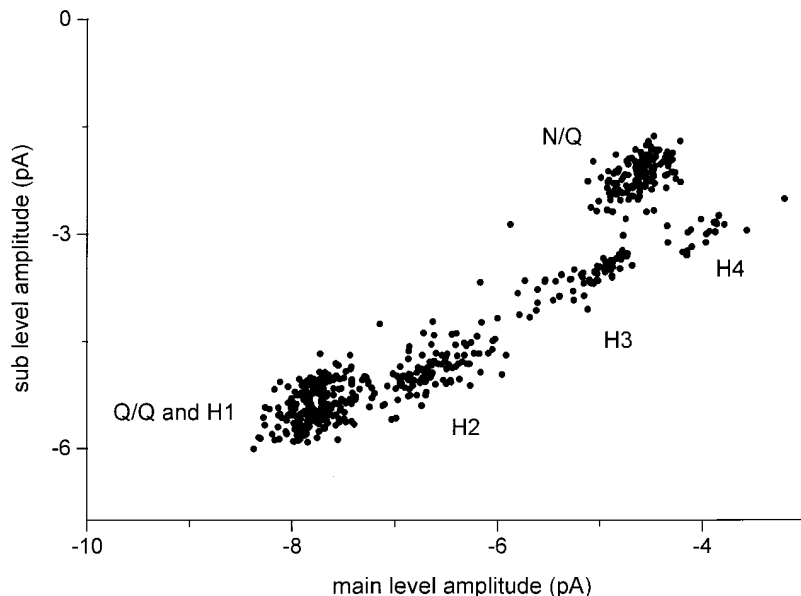sub level amplitude (pA)

main level amplitude (pA)

FIGURE 10. Cluster sub- versus main level amplitudes for mixed NR1 subunit expression. Oocytes were injected with a mixture of wild-type and mutant NR1, plus pure mutant NR2 subunit RNAs. All valid clusters from 10 patches are plotted, irrespective of their classification by pattern. Five groups, from six patterns, are apparent. The group at the lower left is Q/Q plus H1 receptors. The topmost group is N/Q receptors. The hybrid receptor groups (H1, H2, H3, and H4) fall along a diagonal that reflects the 1.4 main/sublevel amplitude ratio. Although there is significant scatter with each group, each population can be distinguished from its neighbors. The properties of these clusters is given in Table III; example clusters and amplitude histograms of each pattern are shown in Fig. 6.

TABLE III

Single-Channel Parameters for Receptors Composed of Pure Mutant NR2 Subunits, and a Mixture of Wild-Type or Mutant NR1 Subunits

		Q/Q	H1	H2	H3	H4	N/Q
	Patches	26	26	22	10	6	23
Amplitude (pA)	i_{main}	-7.67 ± 0.32	-7.60 ± 0.35	-6.66 ± 0.36	-5.36 ± 0.30	-4.36 ± 0.24	-4.58 ± 0.29
	i_{sub}	-5.18 ± 0.42	-5.36 ± 0.26	-4.68 ± 0.36	-3.66 ± 0.24	-3.07 ± 0.26	-2.41 ± 0.19
	i_{closed}	-0.39 ± 0.49	-0.51 ± 0.55	-0.29 ± 0.51	-0.18 ± 0.27	-0.07 ± 0.26	-0.09 ± 0.23
rms noise (pA)	SD_{main}	0.62 ± 0.21	0.59 ± 0.24	0.51 ± 0.20	0.44 ± 0.13	0.45 ± 0.14	0.55 ± 0.12
	SD_{sub}	0.76 ± 0.19	0.68 ± 0.13	0.68 ± 0.16	0.56 ± 0.19	0.45 ± 0.09	0.48 ± 0.12
	SD_{closed}	0.45 ± 0.35	0.62 ± 0.35	0.48 ± 0.31	0.30 ± 0.23	0.27 ± 0.25	0.35 ± 0.17
Occupancy	P_{main}	0.44 ± 0.13	0.19 ± 0.09	0.27 ± 0.16	0.43 ± 0.22	0.38 ± 0.15	0.52 ± 0.17
	P_{sub}	0.46 ± 0.13	0.69 ± 0.12	0.61 ± 0.19	0.48 ± 0.24	0.55 ± 0.17	0.29 ± 0.16
	P_{closed}	0.10 ± 0.13	0.13 ± 0.12	0.12 ± 0.12	0.09 ± 0.11	0.07 ± 0.10	0.19 ± 0.16
Lifetime (ms)	τ_{main}	2.94 ± 1.43	1.89 ± 1.19	2.31 ± 1.44	3.40 ± 2.40	2.51 ± 1.51	3.63 ± 1.99
	τ_{sub}	2.48 ± 1.29	4.39 ± 2.52	4.13 ± 2.76	2.93 ± 1.78	3.31 ± 1.96	2.02 ± 1.66
	τ_{closed}	1.56 ± 2.05	1.50 ± 1.47	1.64 ± 1.59	1.57 ± 1.82	1.34 ± 1.61	2.13 ± 1.77
$-LL/ms$		6.20 ± 0.90	6.10 ± 0.85	5.80 ± 1.20	4.55 ± 0.95	4.25 ± 0.65	4.85 ± 0.80

Oocytes were injected with pure Q NR2 subunits, and a mixture of N and Q NR1 subunits. Six current patterns were observed. All values pertain only to clusters and were estimated using the SKM algorithm (see METHODS). i is the mean amplitude (pA), SD is the noise standard deviation (pA^2), P is the probability of occupying a current level within a cluster, τ is the mean lifetime (ms), and LL is the log likelihood. Values are means $\pm$ SD.

N/Q injections, of 120 clusters, 114 were classified as N/Q, 4 as H4, and 2 as H3. We conclude that for these data–model combinations the separation procedure is ~90% accurate.

The number of clusters of each pattern is not solely dependent on the number of receptors having a specific composition because recording duration varied from patch-to-patch, all patches did not contain receptors of all compositions, and the activation kinetic parameters (which influence the apparent number of events that are counted) are not known and may differ for each receptor subtype. For these reasons, and because the separation procedure was not perfect, the occurrence of each pattern was counted on a patch-by-patch, rather than cluster-by-cluster basis. In this accounting, a pattern was considered to be present in a patch only if >5% of the clusters in that patch were associated with that pattern.

Table IV shows the number of patches having each current pattern as a function of the NR1 Q:N injection ratio. With a 4:1 ratio (7 patches, 461 clusters), the Q/Q, H1, and H2 patterns were observed most frequently, and the N/Q pattern was observed in only one patch. With a 1:1 ratio (14 patches, 1,439 clusters), the Q/Q, H1, and H2 patterns still predominated, but the N/Q pattern was observed in five patches. With either a 1:4 (12 patches, 453 clusters) or a 1:9 injection ratio (11 patches, 526 clusters), the N/Q pattern was most common, but the Q/Q and H1 patterns were still present.

Two general trends can be identified. First, as the Q:N injection ratio is decreased, the relative frequencies of the H1 and H2 patterns decrease and those of H3 and H4 patterns increase. It is therefore probable that H1 and H2 cluster patterns arise from receptors having more Q NR1 subunits, and H3 and H4 patterns arise from receptors having more N NR1 subunits. Second, even at low Q:N ratios, the Q/Q cluster pattern was common (10 of 23 patches). This suggests that receptor assembly is not a random process; i.e., that when the NR2 subunit is a Q, there is a tendency for Q NR1 subunits to coassemble.

For the NR2 mixtures, in 15 patches, 711 clusters were selected, of which 21% were Q/Q, 74% were hy-
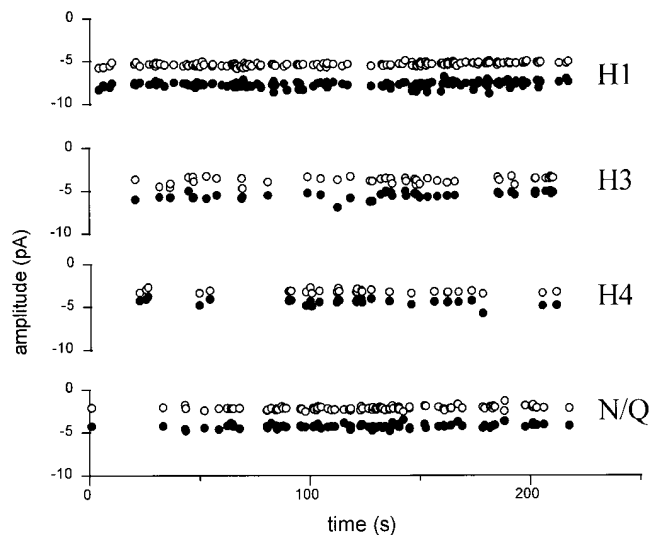

FIGURE 11. Pattern frequency and amplitudes are stable. Clusters of pattern H1, H3, H4, and N/Q were separated using a log likelihood criterion (same patch as in Fig. 9). The sub- (○) and main (●) level amplitudes are plotted for each cluster as a function of time. The results are consistent with four stable populations of receptor in the patch. Main and sublevel amplitudes of each pattern do not drift, and there is no apparent pattern switching or correlation among cluster frequencies of different patterns.
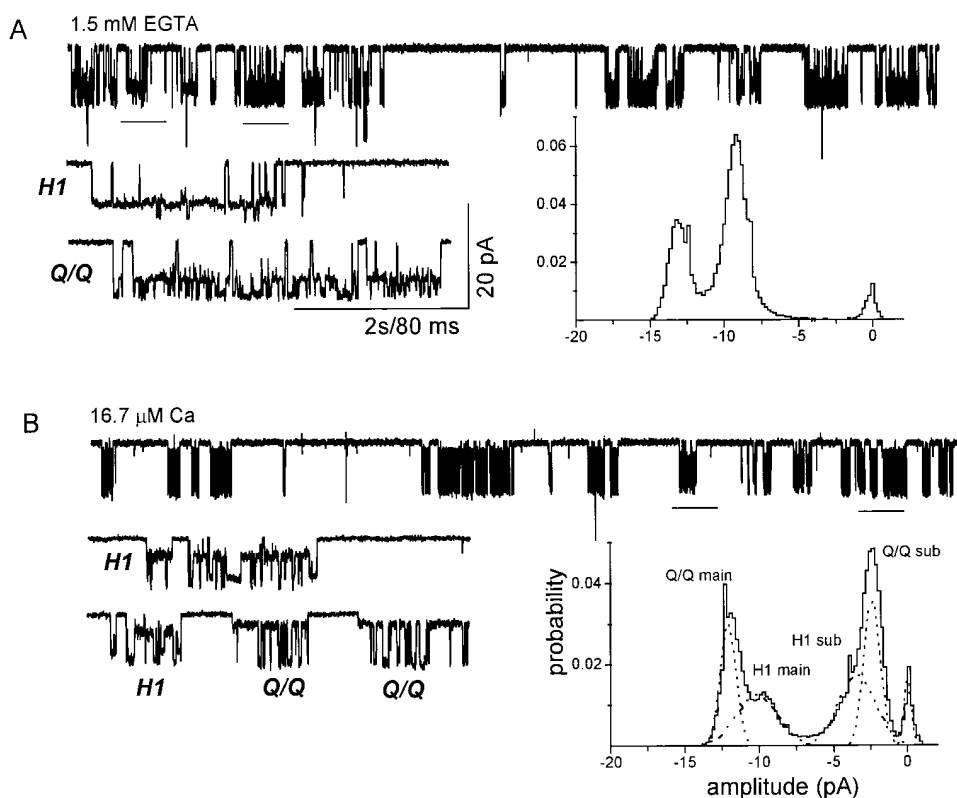
FIGURE 12. Q/Q and H1 receptors respond differently to extracellular Ca^{2+}. Currents are from a single outside-out patch ($V_m = -160$ mV). The oocyte was injected with a 1:1 mixture of wild-type and mutant NR1, plus pure mutant NR2 subunits. Clusters with the Q/Q and H1 patterns were apparent. All traces are continuous. (A) Cluster patterns in Ca^{2+}-free solutions. (*bottom right*) Amplitude histogram of all clusters. The main and sublevel peaks for the Q/Q and H1 patterns overlap in Ca^{2+}-free solution. (B) Cluster patterns in 16.7 μM extracellular Ca^{2+}. Because of channel block by Ca^{2+}, the sublevel of the Q/Q pattern is reduced to −1.0 pA, but the sublevel of the H1 pattern is reduced only to −3.0 pA. (*bottom right*) Amplitude histogram of all clusters. Separate components for main and sublevels of Q/Q and H1 receptors are now resolved in the presence of Ca^{2+}. Note that the H1 pattern appears to have three open channel amplitudes, similar to the NR2 hybrid pattern (Fig. 3). The differential effect of Ca^{++} on the Q/Q and H1 sublevel demonstrates that these patterns arise from distinct receptor populations.

brid, only 2% were N/Q, and 3% were rejects. The relatively high frequency of Q/Q clusters suggests that, as with the NR1 subunit, there appears to be a preferential incorporation of Q NR2 subunits into receptors having all-Q NR1 subunits.

DISCUSSION

We have estimated the number of copies of NR1 and NR2B subunits in recombinant mouse NMDA receptors by counting the number of single-channel current patterns that are observed when mixtures of mutant and wild-type subunits are expressed in oocytes. The central finding is that when both mutant and wild-type NR2B subunits are expressed, three current patterns are observed, and that when both mutant and wild-type NR1 subunits are expressed, six current patterns are observed.

Accuracy of the Pattern Count and Limitations of the Analysis

The numbers of patterns that were observed in mixed subunit injection experiments reflect the numbers of subunit compositions that formed. This accounting will be used to infer NR stoichiometry, and it is therefore important to consider the degree of confidence that can be placed on these values.

The number of patterns was determined independently of the separation procedure. With NR2 subunit mixtures, three distinct cluster patterns (Q/Q, Q/N, and the NR2 hybrid) were observed by direct inspection of the currents. These three patterns were readily identified in patches that had only one pattern (Fig. 3), as well as in all-points amplitude histograms from patches with multiple patterns (Fig. 4). In addition, three groups of amplitudes are evident in scatter plots combined from many patches (Fig. 5), without regard for classification by pattern. In 15 patches in which both Q and N NR2 subunits were injected, only a single NR2 hybrid receptor pattern was observed. In our experiments, when both mutant and wild-type NR2B subunits were expressed, we can be certain that three current patterns were produced.

The case of the NR1 subunit is more complex because there were more patterns, and because the patterns were less distinct. Several lines of evidence support the estimate that six NR1 patterns were produced. (*a*) Single pattern patches. In at least one patch, each of the six patterns was present in isolation of the others (Fig. 6). In addition, all single-pattern patches could be classified according to one of the six patterns of main and sublevel current. Of 44 patches in which both Q and N NR1 subunits were injected, six different patterns were observed in single-pattern patches. (*b*) Consistency of the patterns. The same six patterns that were

TABLE IV

Pattern Frequency, on a Patch-by-Patch Basis, for
NR1 Mixture Experiments

Injection ratio Q:N (NR1)	Q/Q	H1	H2	H3	H4	N/Q	Patches
4:1	0.57	0.57	0.86	0.14	0.00	0.14	7
1:1	0.85	0.79	0.50	0.21	0.14	0.36	14
1:4	0.50	0.50	0.25	0.25	0.08	0.75	12
1:9	0.36	0.45	0.55	0.27	0.27	0.72	11

Oocytes were injected with a mixture of N and Q NR1 subunit RNA, plus all-Q NR2 subunit RNA. Clusters of single-channel current were classified according to pattern using an automated procedure. The probability is the number of patches in which the pattern was observed (in at least 5% of clusters) divided by the total number of patches examined with that injection ratio (last column).

observed in single-pattern patches were also present in patches having multiple patterns. For example, the H1 pattern (main/sublevel amplitudes and occupancy probabilities) was the same in single-, double-, triple-, and quadruple-pattern patches (Figs. 6–9). Similarly, the rarest pattern, H4, was the same in a single-pattern patch (Fig. 6) as in patches having three (Fig. 8) or four (Fig. 9) patterns. The patterns are highly reproducible from patch to patch. (*c*) Grouping of patterns. The clusters fall into six groups, irrespective of their classification into patterns according to likelihood. The scatter plot in Fig. 10 shows all valid clusters; i.e., without regard to their association with a pattern. By eye, five groups are apparent, and, since one group contains two patterns that are distinguished on the basis of relative occupancy of the sublevel (Q/Q and H1), we conclude that there are six patterns.

There are limitations to the conclusions that can be drawn from this accounting, even assuming that the experimentally observed patterns were counted with perfect accuracy. The number of observed patterns would underestimate the number of subunit compositions if some subunit compositions rarely (if ever) assembled. To minimize this possibility, a large number of patches and clusters was examined. Clusters that did not fit any of the test patterns (based on a low likelihood) were found to deviate because of noise or chance overlaps, rather than because they arose from a novel pattern. Nonetheless, it remains possible that more patterns would have been observed if we had examined a larger number of patches and clusters. The number of observed patterns would also underestimate the number of subunit compositions if some subunit compositions produced phenotypes that were not distinguishable. In this case, even a large number of recordings would not aid in their resolution.

Conversely, the number of observed patterns would overestimate the number of subunit compositions if a single assemblage gave rise to variable, or multiple,

phenotypes. For example, we considered that adjacent NR1 patterns (H2/H3 or H3/H4; Fig. 10) might reflect a single distribution with an extraordinary degree of scatter. Several facts argue against this hypothesis. Each pattern was observed in isolation of all others. Given the sparseness of clusters between adjacent pattern groups (Fig. 10), this result would not be expected if the samples were drawn from a single, smeared Gaussian distribution. Moreover, the variance of the NR2 hybrid pattern (Fig. 5 and Table II) is similar to that of pure subunit patterns (Fig. 2 and Table I), so excess variance would necessarily pertain only to the NR1 subunit. With regard to multiple phenotypes, 'modal' behavior was not apparent in receptors having pure mutant or wild-type subunits, nor in the NR2 hybrid. In addition, instances of pattern switching in NR1 hybrid receptors were not observed when the activity level was low (and such events could not be readily attributed to a random overlap of independent clusters), or at longer time scales (Fig. 11). Thus, the results do not suggest that there are more patterns than subunit compositions.

Stoichiometry is essentially a question of structure, and the inference of subunit copy numbers from a purely functional assay such as we have employed cannot be considered definitive. Note that the limitations discussed above apply not only to current pattern analysis, but to other function-based assays of stoichiometry, such as analyses of hybrid receptor pharmacological profiles.

NR1 and NR2B Subunit Copy Numbers

An important result is that a single current pattern was observed when the NR1 or NR2B subunits were purely mutant or wild type. This consistency suggests that all of the expressed receptors have the same number of NR1 and NR2B subunits, and that there is probably a single number of subunits and a single ordering of the NR1 and NR2 subunits in a heteromultimeric receptor. In addition, this result indicates that the properties of the receptors (with regard to current pattern) are stable over the time scale of the recording. The uniformity and stability of the single-channel currents from receptors with unmixed subunits allows novel current patterns that are observed after injection of a mixture of mutant and wild-type subunits to be associated with hybrid receptors having different NR1 and NR2 subunit compositions.

The relationship between the number of observed current patterns in hybrid receptors, and the number of copies of the mutant and wild-type subunits per receptor, depends on the physical mechanisms by which subconductances are generated. These mechanisms are, at present, unknown, so several alternative hypotheses must be considered.

First, a current pattern might be determined only by the number of mutant sidechains at the N_0 position, with no dependence whatsoever on the position(s) of the mutant residue(s) in the receptor. In this case, the number of subunits (n) will be equal to the number of patterns minus 1, with each pattern corresponding to a receptor with 0, 1, . . . n copies of the mutant subunit. According to this hypothesis, the presence of six NR1 and three NR2 patterns would indicate that NMDA receptors are heptamers with the stoichiometry $(NR1)_5$-$(NR2)_2$.

More patterns would be observed if both the number and the positions of the mutant sidechain(s) determine the subconductance pattern. If every positional sequence produced a unique current pattern, there should be 2^n patterns when both N and Q subunits are co-injected, because each of the N residues can be either mutant or wild type. This hypothesis does not fit with the results because the number of observed patterns (six and three) are not powers of two.

Another hypothesis can be considered given that the N_0 residues are likely to encircle the pore, like beads on a necklace. In this case, both the number and position of the mutant sidechains influence the current pattern, but those compositions that superimpose upon rotation, or reflection across a diameter, are considered to be equivalent with respect to current pattern. As a result, fewer than 2^n current patterns would be apparent. Specifically, when each position can have k possible sidechains (in this case two: mutant or wild type), the number of nonequivalent compositions is (Roberts, 1984): $1/2(k^n + k^{n/2})$ if n is even, and $1/2(k^n + k^{(n+1)/2})$ if n is odd.

From these equations we calculate that upon injection of a binary subunit mixture there will be 3 current patterns if there are two copies of the subunit, 6 patterns if there are three copies, and 10 patterns if there are four copies per receptor. The number of patterns that were observed is consistent with this hypothesis if NMDA receptors were pentamers with the stoichiometry $(NR1)_3(NR2B)_2$. Some of the possible compositions are shown in Fig. 13.

The numbers of patterns that were observed are thus consistent with two NMDA receptor stoichiometries: heptamers $[(NR1)_5(NR2)_2]$ or pentamers $[(NR1)_3(NR2B)_2]$. There are few a priori guidelines for selecting between these alternatives because the mechanisms by which mutant sidechains in NMDA receptors influence the amplitude and kinetics of current transitions are not understood. It is even conceivable that the relationship between the number of subunit copies and the number of current patterns could differ for the NR1 and NR2 subunits. However, it is reasonable to speculate that both the number and position of the mutant residues determine the current pattern. The N_0 sidechains form
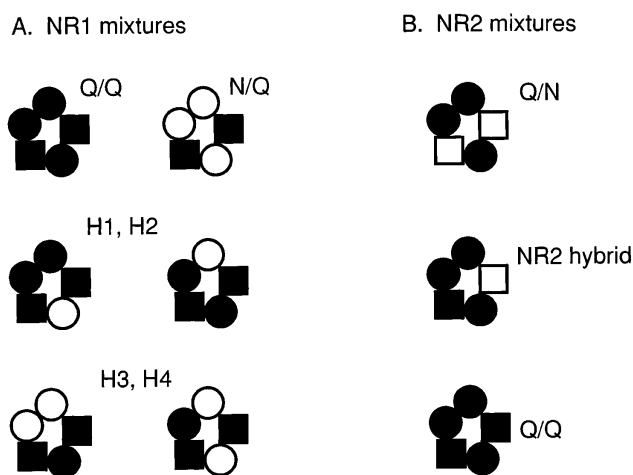

FIGURE 13. Summary of proposed pentameric NMDA receptor stoichiometry. The results are consistent with the presence of three NR1 subunits (*circles*) and two NR2 subunits (*squares*) per receptor (black indicates a mutant subunit). It is assumed that both the number and position of the mutant sidechains influence the current pattern, and that compositions that superimpose upon rotation or reflection across a diameter are equivalent with respect to current pattern. The assemblies are drawn with the NR2 subunits apart, although the experiments do not distinguish whether they are adjacent or apart. (*A*) With three NR1 subunits, six nonequivalent compositions are possible when oocytes are injected with mixed NR1 subunits and pure NR2 subunits. (*top*) The all-mutant NR1 composition has the Q/Q pattern (*left*), and the all-wild-type NR1 composition has the N/Q pattern (*right*). (*middle*) Receptors with one wild-type and two mutant NR1 subunits can assemble with the mutant sidechains adjacent (*left*) or apart (*right*). (*bottom*) Receptors with two wild-type and one mutant NR1 subunit can assemble with the wild-type sidechains adjacent (*left*) or apart (*right*). Based on the results shown in Table IV, H1 and H2 patterns may have two mutant NR1 subunits, and H3 and H4 patterns may have one wild-type NR1 subunit. Example currents from each assembly are shown in Fig. 6. (*B*) With two NR2 subunits, only three nonequivalent compositions are possible when oocytes are injected with pure NR1 and mixed NR2 subunits. These compositions are associated with the Q/N pattern (*top*), the NR2 hybrid pattern (*middle*), and the Q/Q pattern (*bottom*). Example currents from each assembly are shown in Fig. 3.

the narrowest region of the pore (<5.4 A diameter; Villaroel et al., 1995; Wollmuth et al., 1996) and are almost certainly in close contact with each other. It is likely that under such spatially constrained conditions, the single-channel current would be influenced by both the number of mutant and wild-type residues, as well as the types of contacts between the N_0 sidechains. In addition, there is a precedent for both the number and position of mutant sidechains in the pore region influencing the current pattern (Liu et al., 1996).

Biochemical evidence supports a pentameric NMDA receptor stoichiometry. The molecular mass of the immunoprecipitated, cross-linked native NMDA receptor complex is 730 kD, and that of the (glycosylated) NR1 subunit is 116 kD (Brose et al., 1993). The mass of both

NR2A and NR2B subunits, calculated from their sequences, is 163 kD (see Hollman et al., 1994). These subunits are heavily glycosylated, and, if glycosylation increases the molecular mass by ~1.3 kD per site (Brose et al., 1993), the mass of each NR2 subunit would increase to ~185 kD. Given these values, the estimated molecular mass of a fully glycosylated $(NR1)_3$-$(NR2)_2$ pentamer would be 718 kD. Thus, the experimentally determined size of the native NMDA receptors complex is consistent with a $(NR1)_3(NR2)_2$ pentameric stoichiometry.

From these considerations, and from previous studies that suggest that non-NMDA glutamate receptors are pentamers, the most straightforward interpretation of the results is that NMDA receptors are pentamers composed of three NR1 and two NR2 subunits.

Association of Patterns with Compositions

If there are two NR2 subunits per receptor, the single NR2 hybrid pattern can be unambiguously associated with the composition Q_3/QN. For the NR1 subunit, it is less certain how to map the four hybrid patterns (H1–H4) on to the two hybrid compositions (Q_2N/Q_2 and QN_2/Q_2). The H1 and H2 pattern current amplitudes are similar to those of Q_3Q_2 receptors, and the frequency of these hybrid patterns was greater at high Q:N injection ratios (Table IV). Conversely, the H3 and H4 current amplitudes resemble those of N_3Q_2 receptors, and the frequency of these hybrid patterns increased at low Q:N injection ratios. This result suggests that the H1 and H2 patterns arise from receptors having the composition Q_2N/Q_2, and the H3 and H4 patterns with the composition QN_2/Q_2. We speculate that the rather small differences between H1 and H2 (main level amplitude: 7.7 vs. 6.8 pA), and H3 and H4 (main level amplitude: 5.4 vs. 4.1 pA), arise from positional differences rather than a difference in the number of mutant N_0 sidechains. The proposed compositions of the different patterns is summarized in Fig 13.

Given a $(NR1)_3(NR2B)_2$ stoichiometry, there are two possible subunit sequences, with the two NR2 subunits adjacent (1-1-1-2-2) or apart (1-1-2-1-2). (Note that the above discussion regarding the effects of position on the number of current patterns is the same for both alternatives.) The fact that a single pattern is observed in pure mutant or wild-type subunits suggests that a single number and positional sequence of the subunits is imposed during assembly; i.e., that, for all receptors, the NR2 subunits are either adjacent or apart. The assembly of acetylcholine receptor channels, which are pentamers composed of four different subunits, is also not random (Unwin, 1993). We speculated that the large extracellular domains of the acetylcholine and NMDA receptor channel subunits limit and direct the assembly process.

In experiments where the NR2 subunit was all mutant and the NR1 subunit was mixed, incorporation of mutant subunits was still rather common even when the Q:N injection ratio was 1:9 (Table IV). This suggests that there is a preferential incorporation of mutant subunits into receptors; i.e., that the incorporation of an N or a Q subunit is not random and the nature of the N_0 sidechain of the NR1 subunit influences the assembly process.

Comparison with Previous Results

Our results do not agree with previous analyses of subconductance patterns of hybrid NMDA receptors. In similar experiments, using recombinant NR1–NR2A receptors, Behe et al. (1996) observed only one NR1 hybrid pattern and concluded that there are probably two copies of the NR1 subunit per receptor. The reason for the discrepancy with our results is unclear, but may relate to the fact that Behe et al. (1996) expressed the NR1 hybrids on a wild-type NR2 background [(N + R)/N], while we expressed the NR1 hybrids using a mutant NR2 background [(N + Q)/Q]. We observe that subconductance transitions are much less apparent when the NR2 subunit was wild type rather than mutant. In addition, Behe et al. (1996) used receptors having an N-to-R (rather than N-to-Q) mutation. In the presence of 1 mM Ca^{2+}, the sublevel of the R mutant is quite small, and hybrid receptors of different compositions (e.g., with two versus three mutant NR1 subunits) may have current patterns that are not readily distinguishable. Finally, it is possible that with an R mutation, nonrandom assembly and/or right-shifted dose–response profiles may have made some compositions too infrequent to be observed in the number of hybrid patches that were examined.

Wollmuth et al. (1996) determined that substitution of a glycine at the N_0 position of the NR1 subunit or at the structurally homologous N_{+1} position of the NR2 subunit increases the channel diameter to different extents depending on the subunits that are mutated. Mutating all NR1 subunits increases the diameter by 0.20 nm, mutating all NR2 subunits increases it by 0.12 nm, and mutating both NR1 and NR2 subunits increases it by 0.32 nm. These results, obtained by methods that are quite different from single-channel current pattern analysis, are consistent with an NR1:NR2A stoichiometry of 3:2, with an increase in diameter of ~0.065 nm per subunit associated with the Q-to-G mutation.

The results suggest that NMDA receptors, like non-NMDA glutamate receptors (Blackstone et al., 1992; Wenthold et al., 1992; Ferrier-Montiel and Montal, 1996), muscle-type acetylcholine receptors (Toyoshima and Unwin, 1988; Unwin, 1993), neuronal nicotinic acetylcholine receptors (Cooper et al., 1991), glycine receptors (Kuhse et al., 1993), and $GABA_A$ receptors

(Backus et al., 1993; Chang et al., 1996) are composed of five subunits. The narrowest region of the pore of both NMDA (Kuner et al., 1996) and non-NMDA (Hollman et al., 1994) glutamate receptors are formed by a hairpin turn in the M2 segment, similar to the P-loop region of voltage-gated channels. Thus, such a 'loop' motif appears to be present in both tetra- and pentameric channels.

REFERENCES

Backus, K.H., M. Arigoni, U. Drescher, L. Scheurer, P. Malherbe, H. Mohler, and J.A. Benson 1993. Stoichiometry of a recombinant GABA$_A$ receptor deduced from mutation-induced rectification. *Neuroreport.* 5:285–288.

Behe, P., P. Stern, D.J. Wyllie, M. Nassar, R. Schoepfer, and D. Colquhoun 1995. Determination of NMDA NR1 subunit copy number in recombinant NMDA receptors. *Proc. R. Soc. Lond. B Biol. Sci.* 262:205–213.

Benveniste, M., and M.L. Mayer. 1991. Kinetic analysis of antagonist action at *N*-methyl-D-aspartic acid receptors. Two binding sites each for glutamate and glycine. *Biophys. J.* 59:560–573.

Blackstone, C.D., S.J. Moss, L.J. Martin, A.L. Levey, D.L. Price, and R.L. Huganir. 1992. Biochemical characterization and localization of a non-*N*-methyl-D-aspartate glutamate receptor in rat brain. *J. Neurochem.* 58:1118–1126.

Bliss, T.V.P., and G.L. Collingridge 1993. A synaptic model for memory-long-term potentiation in the hippocampus. *Nature (Lond.).* 361:31–39.

Burnashev, N., R. Schoepfer, H. Monyer, J.P. Ruppersberg, W. Gunther, P.H. Seeburg, and B. Sakmann. 1992. Control by asparagine residues of calcium permeability and magnesium blockade in NMDA receptor. *Science (Wash. DC).* 257:1415–1419.

Brose, N., G.P. Gasic, D.G. Vetter, J.M. Sullivan, and S.F. Heinemann. 1993. Protein chemical characterization and immunohistochemical localization of the NMDA receptor subunit NMDAR1. *J. Biol. Chem.* 268:22663–22671.

Chang, Y., R. Wang, S. Barot, and D. Weiss. 1996. Stoichiometry of a recombinant GABA$_A$ receptor. *J. Neurosci.* 16:5415–5424.

Chazot, P.L., S.K. Coleman, M. Cik, and F.A. Stephenson. 1994. Molecular characterization of *N*-methyl-D-aspartate receptors expressed in mammalian cells yields evidence for the coexistence of three subunits types within descrete receptor molecule. *J. Biol. Chem.* 269:24403–24409.

Chung, S.H., J.B. Moore, L. Xia, L.S. Premkumar, and P.W. Gage. 1990. Characterization of single channel currents using digital signal processing techniques based on Hidden Markov Models. *Philos. Trans. R. Soc. Lond. B Biol. Sci.* 329:265–285.

Clark, B.A., M. Farrant, and S.G. Cull-Candy. 1997. A direct comparison of the single-channel properties of synaptic and extrasynaptic NMDA receptors. *J. Neurosci.* 17:107–116.

Clements, J.D., and G.L. Westbrook. 1991. Activation kinetics reveal the number of glutamate and glycine binding sites on the *N*-methyl-D-aspartate receptor. *Neuron.* 7:605–613.

Cooper, E., S. Couturier, and M. Ballivet. 1991. Pentameric structure and subunit stoichiometry of a neuronal nicotinic acetylcholine receptor. *Nature (Lond.).* 350:235–238.

Ferrer-Montiel, A.V., and M. Montal. 1996. Pentameric subunit stoichiometry of a neuronal glutamate receptor. *Proc. Natl. Acad. Sci. USA.* 93:2741–2744.

Forney, G.D. 1973. The "Viterbi algorithm". *Proceedings of the Institute of Electrical and Electronics Engineers.* 61:268–278.

Grimwood, S., B. Le Bourdelles, and P.J. Whiting. 1995. Recombinant human NMDA homomeric NR1 receptors expressed in mammalian cells form a high-affinity glycine antagonist binding site. *J. Neurochem.* 64:525–530.

Hamill, O.P., A. Marty, E. Neher, B. Sakmann, and F.J. Sigworth. 1981. Improved patch-clamp technique for high resolution current recording from cell and cell-free membrane patches. *Pflügers Archiv.* 391:85–100.

Hirai, H., J. Kirsch, B. Laube, H. Betz, and J. Kuhse. 1996. The glycine binding site of the *N*-methyl-D-aspartate receptor subunit NR1: identification of novel determinants of coagonist potentiation on the extracellular M3-M4 loop region. *Proc. Natl. Acad. Sci. USA.* 93:6031–6036.

Hollman, M., and S. Heinemann. 1993. Cloned glutamate receptors. *Annu. Rev. Neurosci.* 17:31–108.

Hollman, M., C. Maron, and S. Heinemann. 1994. *N*-glycosylation site tagging suggests a three domain topology for glutamate receptor GluR1. *Neuron.* 13:1331–1343.

Juang, B.H., and L.R. Rabiner. 1990. The segmental k-means algorithm for estimating parameters of hidden Markov models. *Transaction of Acoustic Speech Signal Processing.* 38:1639–1641.

Kuhse, J., B. Laube, D. Magalei, and H. Betz. 1993. Assembly of the inhibitory glycine receptor: identification of amino acid sequence motifs governing subunit stoichiometry. *Neuron.* 11:1049–1056.

Kuner, T., L.P. Wollmuth, A. Karlin, P.H. Seeburg, and B. Sakmann. 1996. Structure of the NMDA receptor channel M2 segment inferred from the accessibility of substituted cysteines. *Neuron.* 17:343–352.

Kuryatov, A., B. Laube, H. Betz, and J. Kuhse. 1994. Mutational analysis of the glycine-binding site of the NMDA receptor: structural similarity with bacterial amino acid-binding proteins. *Neuron.* 12:1291–1300.

Laube, B., H. Hirai, M. Sturgess, H. Betz, and J. Kuhse. 1997. Molecular determinants of agonist discrimination by NMDA receptor subunits: analysis of the glutamate binding site on the NR2B subunit. *Neuron.* 18:493–503.

Liu, D.T., G.R. Tibbs, and S.A. Siegelbaum. 1996. Subunit stoichiometry of cyclic nucleotide-gated channels and effects of subunit order on channel function. *Neuron.* 16:983–990.

McBain, C.J., and M.L. Mayer. 1994. *N*-methyl-D-aspartic acid receptor structure and function. *Physiol. Rev.* 74:723–760.

Meguro, H., H. Mori, K. Araki, E. Kushiya, T. Kutsuwada, M. Yamazaki, T. Kumanishi, M. Arakawa, K. Sakimura, and M. Mishina. 1992. Functional characterization of a heteromeric NMDA receptor channel expressed from cloned cDNAs. *Nature (Lond.).* 357:70–74.

Methfessel, C., V. Witzemann, T. Takahashi, M. Mishina, S. Numa, and B. Sakmann. 1986. Patch clamp measurement on *Xenopus laevis* oocyte: current through endogenous channels and implanted acetylcholine receptor and sodium channels. *Pflügers Archiv.* 407:577–588.

Monyer, H., R. Sprengel, R. Schoepfer, A. Herb, M. Higuchi, H. Lomelli, N. Burnashev, B. Sakmann, and P.H. Seeburg. 1992. Heteromeric NMDA receptors: molecular and functional distinction of subtypes. *Science (Wash. DC).* 256:1217–1221.

Moriyoshi, K., M. Masu, T. Ishii, R. Shigemoto, N. Mizuno, and S. Nakanishi. 1991. Molecular cloning and characterization of the rat NMDA receptor. *Nature (Lond.).* 354:31–37.

Nakanishi, S. 1992. Molecular diversity of glutamate receptors and implications for brain function. *Science (Wash. DC).* 258:597–603.

Neil, J., Z. Xiang, and A. Auerbach. 1991. List-oriented analysis of single channel data. *Methods Neurosci.* 4:474–490.

Patneau, D.K., and M.L. Mayer. 1990. Structure-activity relationships for amino acid transmitter candidates acting at *N*-methyl-D-aspartate and quisqualate receptors. *J. Neurosci.* 10:2385–2399.

Premkumar, L.S., and A. Auerbach. 1996a. Identification of a high affinity divalent cation binding site near the entrance of the NMDA receptor channel. *Neuron.* 16:869–880.

Premkumar, L.S., and A. Auerbach. 1996b. Stoichiometry of recombinant NMDA receptor channels. *Neuroscience Abstracts.* 22:P593.

Premkumar, L.S., F. Qin, and A. Auerbach. 1997. Subconductance states of a mutant NMDA receptor channel: kinetics and voltage dependence. *J. Gen. Physiol.* 109:181–189.

Qin, F., A. Auerbach, and F. Sachs. 1996b. Idealization of single-channel currents using the segmental k-means method. *Biophys. J.* 70:A227.

Roberts, F.S. 1984. Applied Combinatories. Prentice Hall, Inc., Upper Saddle River, NJ. 307.

Ruppersberg, J.P., J. Mossbacher, W. Gunther, R. Schoepfer, and B. Fakler. 1993. Studying block in cloned *N*-methyl-D-aspartate (NMDA) receptors. *Biochem. Pharmacol.* 46:1877–1885.

Sachs, F. 1983. Automated analysis of single channel records. *In* Single-Channel Recording. B. Sakmann and E. Neher, editors. Plenum Press, New York. 265–285.

Schneggenburger, R., and P. Ascher. 1997. Coupling of permeation and gating in an NMDA-channel pore mutant. *Neuron.* 18:167–177.

Seeburg, P.H. 1993. The molecular biology of mammalian glutamate receptor channels. *Trends Pharmacol. Sci.* 14:297–303.

Sheng, M., J. Cummings, L.A. Roldan, Y.N. Jan, and L.Y. Jan. 1994. Changing subunit composition of heteromeric NMDA receptors during development of rat cortex. *Nature (Lond.).* 386:144–147.

Stern, P., P. Behe, R. Schopfer, and D. Colquhoun. 1992. Single-channel conductances of NMDA receptors expressed from cloned cDNAs: comparison with native receptors. *Proc. R. Soc. Lond. B Biol. Sci.* 250:271–277.

Toyoshima, C., and N. Unwin. 1988. Ion channel of acetylcholine receptor reconstructed from images of postsynaptic membranes. *Nature (Lond.).* 336:247–250.

Unwin, N. 1993. Nicotinic acetylcholine receptor at 9 A resolution. *J. Mol. Biol.* 229:1101–1124.

Villarroel, A., N. Burnashev, and B. Sakmann. 1995. Dimensions of the narrow portion of a recombinant NMDA receptor channel. *Biophys. J.* 68:866–875.

Wenthold, R.J., N. Yokotani, K. Doi, and K. Wada. 1992. Immunohistochemical characterization of the non-NMDA glutamate receptor using subunit specific antibodies. Evidence for a hetero-oligomeric structure in rat brain. *J. Biol. Chem.* 267:501–507.

Wollmuth, L.P., T. Kuner, P.H. Seeburg, and B. Sakmann. 1996. Differential contribution of the NR1- and NR2A-subunits to the selectivity filter of recombinant NMDA receptor channels. *J. Physiol.* 491:779–797.